2017

Evaluation of fertilizer-drawn forward osmosis for coal seam gas reverse osmosis brine treatment and sustainable agricultural reuse

Youngjin Kim
Korea University, University of Technology Sydney

Yun Chul Woo
University of Technology Sydney

Sherub Phuntsho
University of Technology Sydney

Long D. Nghiem
University of Wollongong, longn@uow.edu.au

Ho Kyong Shon
University of Technology Sydney, hkshon@enguts.edu.au

See next page for additional authors

Evaluation of fertilizer-drawn forward osmosis for coal seam gas reverse osmosis brine treatment and sustainable agricultural reuse

Abstract

The fertilizer-drawn forward osmosis (FDFO) was investigated for treating coal seam gas (CSG) produced water to generate nutrient rich solution for irrigation. Its performance was evaluated and compared with reverse osmosis (RO) in terms of specific energy consumption (SEC) and nutrient concentrations in the final product water. The RO-FDFO hybrid process was developed to further improve FDFO. The results showed that FDFO has the lowest SEC followed by the RO-FDFO and RO processes. The final nutrient concentration simulation demonstrated that the RO-FDFO hybrid process has lower final concentration, higher maximum recovery and lower nutrient loss than the stand alone FDFO process. Therefore, it was suggested that the RO-FDFO is the most effective treatment option for CSG produced water as well as favourable nutrient supply. Lastly, membrane fouling mechanism was examined in CSG RO brine treatment by FDFO, and the strategies for controlling fouling were critically evaluated. KNO3 exhibited the highest flux decline corresponding to the highest reverse salt flux, while the most severe membrane scaling was observed with calcium nitrate, primarily due to the reverse transport of calcium ions. To control membrane fouling in FDFO process, both physical flushing and chemical cleaning were examined. Membrane cleaning with citric acid of 5% resulted in a complete flux recovery.

Disciplines

Engineering | Science and Technology Studies

Publication Details

Kim, Y., Woo, Y. Chul., Phuntsho, S., Nghiem, L. D., Shon, H. & Hong, S. (2017). Evaluation of fertilizer-drawn forward osmosis for coal seam gas reverse osmosis brine treatment and sustainable agricultural reuse. Journal of Membrane Science, 537 22-31.

Authors

Youngjin Kim, Yun Chul Woo, Sherub Phuntsho, Long D. Nghiem, Ho Kyong Shon, and Seungkwan Hong

Evaluation of fertilizer-drawn forward osmosis for coal seam gas reverse osmosis brine treatment and sustainable agricultural reuse

Youngjin Kim [a, b], Yun Chul Woo [b], Sherub Phuntsho [b], Long D. Nghiem [c], Ho Kyong Shon [b*], Seungkwan Hong [a*]

[a] School of Civil, Environmental and Architectural Engineering, Korea University, 1-5 Ga, Anam-Dong, Seongbuk-Gu, Seoul, 136-713, Republic of Korea

[b] Centre for Technology in Water and Wastewater, School of Civil and Environmental Engineering, University of Technology Sydney (UTS), Post Box 129, Broadway, NSW 2007, Australia

[c] Strategic Water Infrastructure Laboratory, School of Civil Mining and Environmental Engineering, University of Wollongong, Wollongong, NSW 2522, Australia

[*] Co-corresponding authors.

Hokyong Shon. Tel.: +61-2-9514-2629; E-mail: Hokyong.Shon-1@uts.edu.au

Seungkwan Hong. Tel.: +82-2-3290-3322; E-mail: skhong21@korea.ac.kr

Abstract

The fertilizer-drawn forward osmosis (FDFO) was investigated for treating coal seam gas (CSG) produced water to generate nutrient rich solution for irrigation. Its performance was evaluated and compared with reverse osmosis (RO) in terms of specific energy consumption (SEC) and nutrient concentrations in the final product water. The RO-FDFO hybrid process was developed to further improve FDFO. The results showed that FDFO has the lowest SEC followed by the RO-FDFO and RO processes. The final nutrient concentration simulation demonstrated that the RO-FDFO hybrid process has lower final concentration, higher maximum recovery and lower nutrient loss than the stand alone FDFO process. Therefore, it was suggested that the RO-FDFO is the most effective treatment option for CSG RO brine as well as favorable nutrient supply. Lastly, membrane fouling mechanism was examined in CSG RO brine treatment by FDFO, and the strategies for controlling fouling were critically evaluated. KNO_3 exhibited the highest flux decline corresponding to the highest reverse salt flux, while the most severe membrane scaling was observed with calcium nitrate, primarily due to the reverse transport of calcium ions. To control membrane fouling in FDFO process, both physical flushing and chemical cleaning were examined. Membrane cleaning with citric acid of 5% resulted in a complete flux recovery.

Keywords: CSG produced water, Fertilizer-drawn forward osmosis, Specific energy consumption, FDFO simulation, Membrane cleaning.

44

Nomenclature

A	Water permeability coefficient
B	Salt permeability coefficient
$C_{D,i}$	Maximum DS concentration
$C_{D,f}$	Final DS concentration having equal osmotic pressure with the initial FS concentration
$C_{nut,f}$	Nutrient concentration in the final produced water
J_s	Reverse salt flux
J_w	Water flux
$Loss_{Draw}$	Draw solute loss at the maximum recovery rate in FDFO
M_w	Molecular weight of DS
n	Number of species
P_D	Draw pressure (bar)
P_F	Feed pressure (bar)
Q_D	Draw flow rate (m^3/h)
Q_F	Feed flow rate (m^3/h)
$Q_{P,FDFO}$	Permeate flow rate (m^3/h) in FDFO
$Q_{P,RO}$	Permeate flow rate (m^3/h) in RO
$Q_{P,total}$	Total permeate flow rate (m^3/h)
$Ratio_{nut}$	Ratio of each nutrient component

R_{max}	Maximum recovery rate in FDFO
R_g	Universal gas constant
S	Structure parameter of the support layer
SEC_{FDFO}	Specific energy consumption of FDFO
SEC_{RO}	Specific energy consumption of RO
$SEC_{RO+FDFO}$	Specific energy consumption of the RO-FDFO hybrid process
$SRSF$	Specific reverse salt flux
T	Temperature
$V_{D,i}$	Initial DS volume
$V_{D,f}$	Final DS volume
V_{ext}	Water extraction capacity

Greek symbol

η	Pump efficiency

Abbreviation

CAN	Calcium nitrate
CSG	Coal seam gas
DAP	Di-ammonium phosphate

87	DI	Deionized
88	DS	Draw solution
89	EDTA	Ethylenediaminetetraacetic acid
90	EDX	Energy dispersive x-ray spectroscopy
91	FDFO	Fertilizer-drawn forward osmosis
92	FO	Forward osmosis
93	FS	Feed solution
94	FSF	Forward salt flux
95	ICP	Internal concentration polarization
96	NF	Nanofiltration
97	OMBR	Osmotic membrane bioreactor
98	PA	Polyamide
99	RO	Reverse osmosis
100	SEM	Scanning electron microscopy
101	SOA	Ammonium sulphate
102	RSF	Reverse salt flux
103	SEC	Specific energy consumption
104	SRSF	Specific reverse salt flux
105	TFC	Thin-film composite
106	XRD	X-Ray diffraction
107		

1. Introduction

Coal seam gas (CSG), which is also known as coal-bed methane, has been widely explored in United States, Australia, Canada, United Kingdom, and other nations since the 1970s [1]. During CSG extraction, underground water in the coal seam is pumped to the surface together with methane gas. This is often called CSG produced water, which is dominantly composed of sodium, chloride and bicarbonate [2]. In Australia, the salinity of CSG produced water is relatively low, typically in the range of up to 6,000 mg/L [3]. Thus, CSG produced water can be treated and utilized for a variety of application including irrigation [4]. Since CSG produced water has a high sodium content (i.e. a high sodium adsorption ratio), utilization of untreated CSG produced water for irrigation can lead to a gradual decrease in the permeability of soil, eventually causing infiltration problems and other form of soil degradation [5]. Therefore, it is necessary to remove sodium to enable reuse of CSG produced water for irrigation.

Reverse osmosis (RO) is currently the most widely used technology for CSG produced water treatment (**Fig. 1a)** due to its several merits such as small footprint, ease of automation, and modular design [6]. However, RO generally exhibits high energy consumption (i.e., typically above 4-5 kWh/m^3 for a seawater desalination plant) due to the high hydraulic pressure as a driving force [7]. Moreover, RO is often hampered by high fouling potentential and inherent limitations such as low recovery [8, 9]. To overcome these issues, forward osmosis (FO) was proposed since it can provide high rejection of contaminants, low fouling propensity, high fouling reversibility and low energy requirement [10, 11]. However, FO has several limitations including the need to extract

pure water from the diluted draw solution (DS), requiring the additional desalting processes (e.g., nanofiltration (NF), RO or membrane distillation) [12, 13].

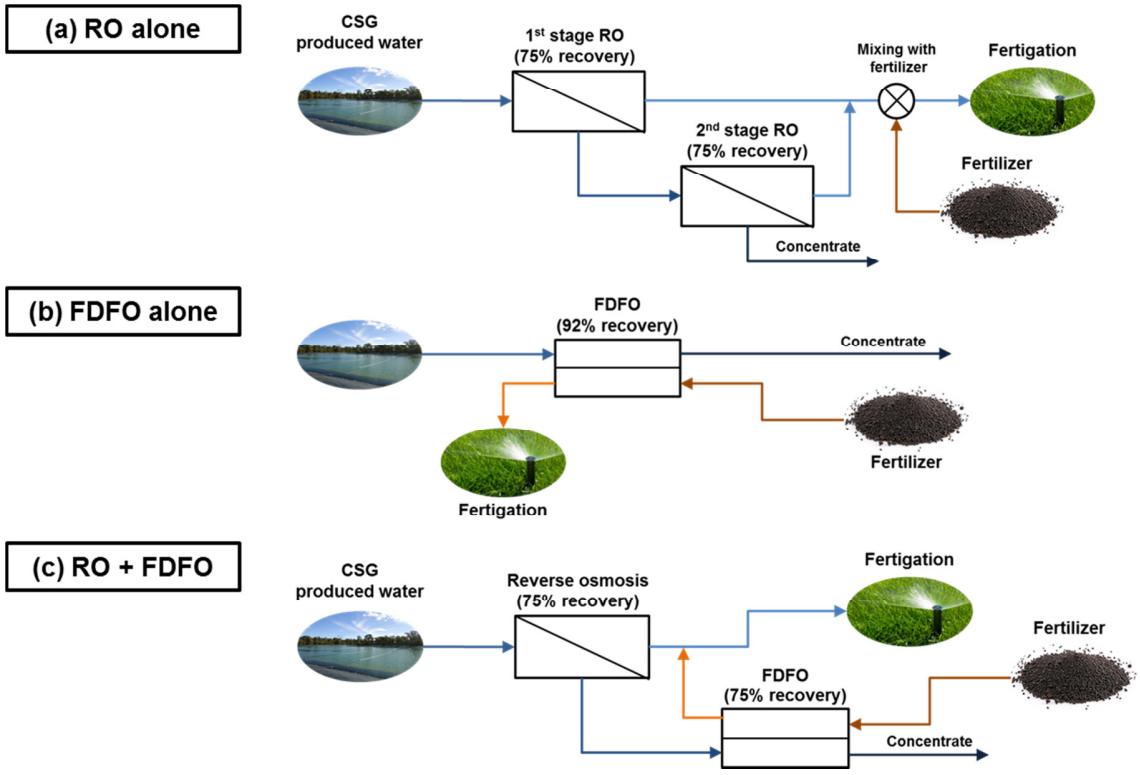

Figure 1. Conceptual process layout for integrating RO-FDFO hybrid process: (a) 2 stage RO system, (b) FDFO alone system and (c) RO-FDFO hybrid system.

Recently, fertilizer-drawn forward osmosis (FDFO) has received increased attention since the diluted fertilizer solution can be utilized directly for irrigation purpose and thus the diluted DS separation and recovery process is not required [14-16]. However the diluted fertilizer solution still required substantial dilution since the final nutrient concentration can exceed the standard nutrient requirements for irrigation especially using feed water sources

142 with high salinity [15, 16]. Thus, NF can be employed as a post-treatment process for
143 further dilution and in meeting the water quality requirements for fertigation [14]. However,
144 FDFO is seen to be more suitable for the treatment of low salinity impaired water sources
145 (e.g., CSG produced water, wastewater and so on) as shown in **Fig. 1b** so that desired
146 fertilizer dilution can be achieved without the need of a NF post-treatment process [17].

147 Since FDFO utilizes highly concentrated fertilizer DS, FDFO has serious problems
148 regarding the reverse solute flux of the draw solute induced by the large concentration
149 differences between the feed solution (FS) and DS across FO membrane. The reverse
150 diffusion of draw solutes to FS in the FDFO process can reduce the recovery rate and lose
151 the valuable fertilizers in DS. In addition, reverse salt flux (RSF), which is reversely
152 diffused draw solute through FO membrane from DS to FS, can alter the feed chemistry
153 and accelerate membrane fouling or scaling [18-20], and inhibit the biological processes in
154 osmotic membrane bioreactor (OMBR) which is one of the potential applications [17, 21].
155 Moreover, because of an increase in FS concentration caused by RSF, direct discharge of
156 FS may entail negative impacts to the environment [22], which requires further treatment of
157 FS concentrate.

158 In order to solve or mitigate these problems (i.e., high energy consumption in RO
159 and valuable fertilizer draw solute loss by RSF in FDFO), a RO-FDFO hybrid process was
160 proposed for simultaneous CSG produced water treatment for the agricultural application
161 based on the concept described in **Fig. 1c**. This hybrid system consists of two parts (i.e.,
162 RO and FDFO). The 1st stage RO will concentrate CSG produced water by up to 75% and
163 produce clean water. Then, the 2nd stage FDFO will treat CSG RO brine from the 1st stage

RO and also produce nutrient solution. The diluted fertilizer DS from the FDFO process will be mixed with RO permeate and supplied for fertigation. In this system, CSG produced water will be utilized as an influent and a highly concentrated fertilizer solution will be used as DS for the RO-FDFO hybrid process. The diluted fertilizer solution can then be obtained and supplied to fertigation.

Therefore, this study aims to evaluate the feasibility of the RO-FDFO hybrid system for the treatment of CSG produced water and production of nutrient solution by comparing with RO alone and FDFO alone. Comparisons are made based on the specific energy consumptions (SEC) and nutrient concentrations in the final FDFO product water. Finally, membrane scaling and fouling in FDFO during CSG RO brine treatment was evaluated and the cleaning strategies were further investigated using both physical cleaning and chemical cleaning.

2. Materials and methods

2.1 FO membrane and draw solutions

FO membrane used in this study was provided by Toray Chemical Korea (South Korea). This membrane was a thin-film composite (TFC) polyamide (PA) FO membrane with an embedded woven mesh for mechanical strength as shown in **Fig. S1**. The total membrane thickness was approximately 60 μm. The intrinsic FO membrane characteristics (i.e., the water permeability coefficient (A) and the salt permeability coefficient (B) of the active layer, and the structure parameter (S) of the support layer) were detemined based on

185 the mathematical method [23] and shown in **Table S1**. For storage, the membranes were
186 immersed in deionized (DI) water at 4 °C and the water was replaced regularly.

187 Four different reagent grade chemical fertilizers (i.e., ammonium sulphate (SOA),
188 calcium nitrate (CAN), di-ammonium phosphate (DAP), potassium nitrate (KNO_3)) (Sigma
189 Aldrich, Australia) were used as draw solutes. DS was prepared by dissolving fertilizer
190 chemicals in DI water. Detailed information of fertilizer chemicals is provided in **Table S2**.
191 Osmotic pressure and diffusivity of four fertilizers were obtained by OLI Stream Analyzer
192 3.2 (OLI System Inc., Morris Plains, NJ, USA).

193

194 **2.2 Coal seam gas reverse osmosis brine**

195 CSG RO brine used in this study was from a RO pilot plant treating CSG produced
196 water from Gloucester Basin in the Upper Hunter, New South Wales, Australia. Operation
197 conditions of the pilot plant were as follows: ultrafiltration pre-treatment, 5 mg/L
198 antiscalant (Osmotreat, Osmoflo, Adelaide, South Australia, Australia), and RO recovery of
199 75% [2]. Detail information of CSG RO brine used as FS in this study is provided in **Table**
200 **1**.

201

202 **Table 1.** Water quality of CSG RO brine used in this study. CSG RO brine was collected
203 from a pilot-scale RO system for treating CSG produced water from the Gloucester gas
204 field [24].

General	Values	Ion concentration	Values

characteristics			
pH	9.07	SO_4^{2-} (mg/L)	23.3 ± 3.1
Conductivity (mS/cm)	22.58 ± 0.02	PO_4^{3-} (mg/L)	5.21 ± 0.17
Total dissolved solids, TDS (mg/L)	15,354 ± 12	Cl^- (mg/L)	4,793 ± 87
Alkalinity (mg/L $CaCO_3$ equivalent)	6,467 ± 58	Na^+ (mg/L)	6,089 ± 48
Water hardness (mg/L $CaCO_3$ equivalent)	151 ± 1	K^+ (mg/L)	28.7 ± 0.6
Sodium absorption ratio (SAR)	215.3 ± 1.2	Ca^{2+} (mg/L)	36.3 ± 0.6
Turbidity (NTU)	1	Mg^{2+} (mg/L)	14.7 ± 0.6
		Si (mg/L)	23.5 ± 0.9

205

206 ## 2.3 Fertilizer-drawn forward osmosis experiments

207 ### 2.3.1 Fertilizer-drawn forward osmosis experiments

208 All FDFO experiments were carried out using a lab-scale FO system similar to the
209 one described in our previous studies [25]. The FO cell had two symmetric channels
210 consisting of 77 mm long, 26 mm wide and 3 mm deep on both sides of the membrane each
211 for each FS and DS. Variable speed gear pumps (Cole-Parmer, USA) were used to provide
212 crossflows under counter-current directions at a crossflow rate of 8.5 cm/s and solution
213 temperature of 25 ± 1 °C. All FDFO operations were carried out using 1 M fertilizers as DS
214 and CSG RO brine as FS under the AL-FS (i.e., active layer facing FS) mode of membrane
215 orientation. Both solutions were recirculated in a closed-loop system resulting in a batch
216 mode process operation. The DS tank was placed on a digital weighing scale and the weight
217 changes were recorded by a computer in real time every 3 minutes interval to determine the
218 water flux. Conductivity and pH meters (HACH, Germany) were connected to a computer
219 to monitor concentration and pH changes in the feed tank.

220 ### 2.3.2 Physical cleaning

221 In order to investigate the effect of physical cleaning on water flux recovery of the
222 FO membrane after fouling, two different physical cleaning methods (i.e., hydraulic
223 washing and osmotic backwashing) were adopted for all FDFO experiments. Hydraulic
224 washing consisted of flushing DI water inside the DS and FS channels at 3 times higher
225 crossflow velocity (25.5 cm/s) for 30 minutes. Osmotic backwashing was conducted for 30
226 minutes by flushing 1M NaCl DS solution on the active layer side of the membrane and DI
227 water on the support layer side (both at 8.5 cm/s crossflow velocity) (AL-DS mode of

membrane orientation) in order to provide water flux in reverse direction to the fouling experiments. Water recovery rate was determined by comparing the baseline water flux of the virgin FO membrane conducted before the CSG RO brine treatment and after the physical cleaning using 1M NaCl as DS and DI as FS.

2.3.3 Chemical cleaning

To investigate the effect of chemical cleaning on water flux recovery, three different chemical cleaning agents (1 mM ethylenediaminetetraacetic acid (EDTA) [26], 1 mM sodium hydroxide (NaOH) [27] and 1-5% citric acid [28]) were adopted. Chemical cleaning consisted of flushing a cleaning agent inside the FS channel and DI water inside the DS channel at the same crossflow velocity (8.5 cm/s) for 30 minutes. Water recovery rate was determined by comparing the baseline water fluxes of the virgin FO membrane and membrane after chemical cleaning using 1M NaCl as DS and DI as FS.

2.4 Membrane surface characterization

The surfaces of FO membranes were observed and analysed by scanning electron microscopy (SEM, Zeiss Supra 55VP, Carl Zeiss AG, Germany) and energy dispersive X-ray spectroscopy (EDX) following the procedures described in a previous study [29]. Samples taken from each membrane were first lightly coated with Au/Pd. The SEM imaging was carried out at an accelerating voltage of 10 kV and multiple image magnifications at various areas were taken for each sample.

X-Ray diffraction (XRD) (Siemems D5000, USA) analysis was also performed over Bragg angles ranging from 10° to 60° (Cu Kα, λ=1.54059 Å) to investigate the dominant species responsible for scaling formed on the membrane surface. Membrane samples

collected after experiments were first soaked in DI water for a few minutes to remove any feed or draw solutes and then dried in a desiccator for 1 day before SEM imaging was measured.

2.5 Specific energy consumption (SEC) estimation

Energy consumptions of the three processes (i.e., RO, FDFO and RO-FDFO hybrid process) were estimated in terms of SEC. ROSA 9.1 software (DOW FILMTEC, USA) was used to estimate SEC of RO alone. SEC of the FDFO standalone process was estimated based on the following equiation [30]:

$$SEC_{FDFO} = \frac{P_F Q_F + P_D Q_D}{36 \times \eta \times Q_P} \quad (1)$$

where, P_F is the feed pressure (bar), P_D is the draw pressure (bar), Q_F is the feed flow rate (m^3/h), Q_D is the draw flow rate (m^3/h), Q_P is the permeate flow rate (m^3/h) and η is the pump efficiency. The total SEC in the RO-FDFO hybrid process is the sum of the energy consumption as shown in **Eq. (2).**

$$SEC_{RO+FDFO} = \frac{SEC_{RO} Q_{P,RO} + SEC_{FO} Q_{P,FD\,FO}}{Q_{P,total}} \quad (2)$$

where, $Q_{P,total}$, $Q_{P,RO}$ and $Q_{P,FDFO}$ are the total permeate flow rate (m^3/h), the permeate flow rate (m^3/h) in RO and the permeate flow rate (m^3/h) in FDFO, respectively. It should be noted here that, for SEC estimation of both RO and FDFO, RO membrane, FS, the pump efficiency and the feed and draw pressure in FDFO alone were assumed to be BW30-4040 (Dow Filmtec, USA), CSG produced water [2], 80% and 1 bar, respectively. BW30-4040 is a brackish water RO membrane with high salt rejection. If CSG produced water contains

high concentration of organics, the viscosity will be seriously increased as the CSG produced water is concentrated, which can result in a significant reduction in the pump efficiency. However, since CSG produced water has quite low concentration of organics (e.g., 1.7 mg/L TOC) [2], the pump efficiency can be assumed to be constant as 80%.

2.6 Final nutrient concentration simulation

Nutrient concentrations in the final product water can be simulated using the water extraction capacity (V_{ext}) of 1 kg DS [15, 31]. This equation was derived under counter – current crossflow mode with an assumption of no forward salt flux (FSF) and no RSF.

$$V_{ext} = \frac{1000}{M_w}\left[\frac{1}{C_{D,i}} - \frac{1}{C_{D,f}}\right] \quad (3)$$

where, M_w is molecular weight of DS, $C_{D,i}$ is the maximum DS concentration (solubility) and $C_{D,f}$ is the final DS concentration having equal osmotic pressure with the initial FS concentration. In the FO process, RSF could have a significant impact on the FO process by increasing the FS concentration and decreasing the DS concentration, resulting in lower effective osmotic driving force. However, the effect of RSF on the FDFO process was not considered for **Eq. (3)** and thus, the water extraction capacity by **Eq. (3)** is likely to be over-estimated. In this study, therefore, **Eq. (3)** was modified by adopting the definition of specific reverse salt flux (SRSF) as follows.

$$V_{ext} = \frac{1-\left(\frac{C_{D,f}}{C_{D,i}}\right)}{\left(\frac{C_{D,f}M_w}{1000}\right)+SRSF} \quad (4)$$

where SRSF is defined as the ratio of RSF to water flux in the FO process as presented in **Eq. (5)**. The SRSF is independent of membrane support layer properties and

can quantitatively elucidate FO membrane performance [25]. Here, we assumed that SRSF is constant without any change even though membrane fouling occurs during operation.

$$\frac{J_s}{J_w} = \frac{B}{A}\frac{1}{nR_gT} \quad (5)$$

where, n is the number of species that the draw solute dissociates into, A is the water permeable coefficient, B is the salt permeable coefficient, R_g is the gas constant, and T is the temperature. Nutrient concentrations in the final produced water can be obtained by using **Eq. (6)**. This equation was derived from mass balance for draw solute.

$$C_{nut,f} = \frac{1-SRSF\times V_{ext}}{V_{D,f}} \times Ratio_{nut} \quad (6)$$

where, $Ratio_{nut}$ is the ratio of each nutrient component and $V_{D,f}$ is the final DS volume. Based on **Eq. (4)**, the draw solute loss and the maximum recovery rate of FDFO can be also obtained as **Eq. (7)** and **Eq. (8)**, respectively.

$$Loss_{Draw} = \frac{SRSF\times V_{ext}}{C_{D,i}V_{D,i}} \times 100\% \quad (7)$$

$$R_{max} = \frac{Q_F - V_{ext}}{Q_F} \quad (8)$$

where, $Loss_{Draw}$ is the draw solute loss at the maximum recovery rate in FDFO, $V_{D,i}$ is the initial DS volume and R_{max} is the maximum recovery rate in FDFO.

3. Results and discussion

3.1 Specific energy consumption simulation of reverse osmosis, fertilizer-drawn forward osmosis and reverse osmosis – fertilizer-drawn forward osmosis hybrid processes for coal seam gas produced water treatment

The simulated SECs of the three processes (i.e., RO, FDFO and RO-FDFO hybrid processes) for treating CSG produced water and the supplying nutrient solution for irrigation are presented as a function of feed recovery rates (%) in **Fig. 2**. The efficiency of the high pressure pump for RO and the circulation pump for FDFO was assumed at 80% and the applied pressure for circulating FS and DS in FDFO was set at 1 bar [30].

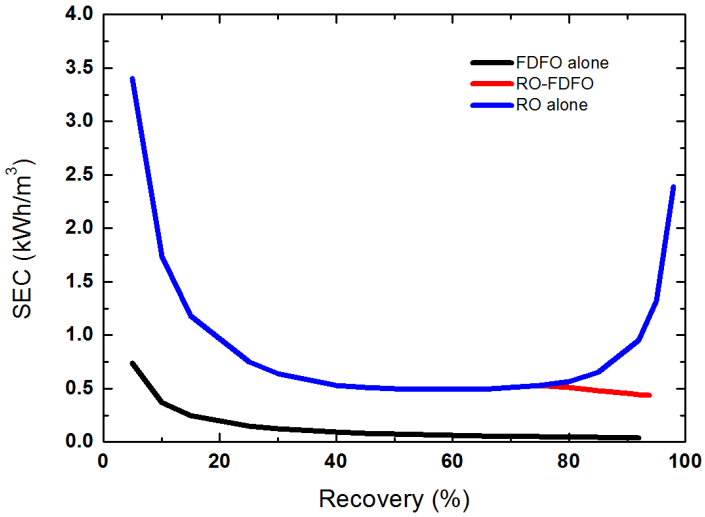

Figure 2. SEC evaluation of RO alone, FDFO alone and RO-FDFO hybrid processes as a function of recovery rate (%). The estimated SEC results are defined as overall energy consumption (kWh) per produced water (m^3). The flow rate in FS for all processes and the working pressure for FDFO operation were assumed to be 20 m^3/d and 1 bar, respectively.

The pump efficiency was assumed to be 80%. Osmotic pressures of CSG produced water and RO brine at 75% recovery were 2.46 bar and 11.64 bar, respectively.

In RO alone, the SEC significantly reduced from 3.5 kWh/m^3 to 0.7 kWh/m^3 by increasing the feed recovery rate of up to 75% beyond which the SEC started to increase rapidly. This is due to the significant increase in hydraulic pressure needed to overcome the increased osmotic pressure of the feed concentrate along the fee channel. For example, osmotic pressure increases 4 times when recovery rate reaches up to 75% against 2 times increase at 50% recovery rate. The reults in **Fig 2** indicates that, the osmotic pressure of feed concentrate increases exponentially with the recovery rates above 75% thereby signficantly increasing the hydraulic pressure needed to overcome this enhanced osmotic pressure.

The SEC of the FDFO process alone shows that, the SEC continuously reduced with increasing recovery rate. In the RO process, the hydraulic driving force incresed with the recovery rates due to increase in the the osmotic pressure of the feed and its concentrate thereby incresaing the SEC. However, in the FDFO process, the driving force and the feed recovery rates can be simply increased by increasing the initial DS concentration without impacting the hydraulic pressure and SEC of the process [32]. Consequently, FDFO has much lower SEC than RO due to its lower hydraulic operatiing pressure, consistent with other studies [30, 33].

Lastly, FDFO was combined with RO as shown in **Fig. 1c** to increase the overall feed recovery rate without signficantly impacting on the SEC. As discussed above, when

343 the RO process is used alone, it was found that SEC increased rapidly with feed recovery
344 rates above 75% . When FDFO is combined with RO for the treatment of its brine after 75%
345 recovery rate, the overall recovery rate can be signficantly increased without much impact
346 on the total energy consumption or the combined SEC. Simulation results showed that SEC
347 of the RO-FDFO combined process continuously decreased even up to 95% recovery rate.
348 Based on all the SEC simulation results above, it can be concluded that FDFO alone is the
349 most economic process followed by the RO-FDFO hybrid process and RO alone.
350

351 ### 3.2 Comparison of final nutrient (N/P/K) concentration between fertilizer-drawn
352 forward osmosis and reverse osmosis – fertilizer-drawn forward osmosis hybrid
353 processes

354 The RO process alone produces pure water with a quality that is generally suitable
355 for direct irrigation with or without remineralisation. Since the FDFO process alone does
356 not generate pure water, their final water quality must be assessed against key irrigation
357 criteria. For comparison, FDFO alone and the RO-FDFO hybrid process were selected and
358 compared in terms of final nutrient concentration, draw solute loss, and maximum recovery
359 rate.

360 Before the simulation, SRSF was experimentally measured and presented in **Table.**
361 **S3**. Results show that SOA had the lowest SRSF followed by DAP, CAN and KNO_3. With
362 regards to water flux, KNO_3 showed the highest water flux followed by SOA, CAN and
363 DAP, which is not consistent with osmotic pressures of fertilizers (**Table S2**). This
364 difference in water flux between fertilizers is explained from the variations of the extent of

365 ICP effects induced by the mass transfer resistance (K) within the membrane support layer.
366 Since mass transfer resistance refers to the ratio between the *S* parameter and diffusivity of
367 DS, a draw solute with higher diffusivity has low mass transfer resistance and should have
368 high water flux [17, 25]. In terms of RSF, SOA exhibited the lowest RSF followed by DAP,
369 CAN and KNO_3. Unlike the water flux, the trend for RSF with diffusivity was quite
370 different. This is because RSF is theoretically a function of not only the effective
371 concentration gradient across the active layer of the FO membrane but also the salt
372 rejecting properties of the membrane [17, 34]. As a consequence, SRSF of fertilizer DS was
373 determined by the salt permeable coefficient (B value) which varies with fertilizers. From
374 these results, it can be drawn that SOA is possibly the optimum fertilizer DS in terms of
375 draw solute loss and maximum recovery rate since it has the smallest draw solute loss with
376 the same volume of feed water extraction.

377 The draw solute loss and the maximum recovery rate of both FDFO and RO-FDFO
378 hybrid processes were firstly simulated using **Eq. (7)** and **Eq. (8)**, respectively and
379 presented in **Fig. 3**. As expected, in FDFO process, KNO_3 exhibited the highest draw solute
380 loss followed by DAP, CAN and SOA (**Fig. 3a**). It is interesting to note that DAP showed
381 higher draw solute loss than CAN in spite of its lower SRSF. This is because the draw
382 solute loss is affected by both the extraction capacity and SRSF as shown in **Eq. (7)**,
383 indicating that higher extration capacity of DAP also induced higher draw solute loss.
384 Results of **Fig. 3b** indicated that maximum recovery rates of both processes have the totally
385 a different trend with SRSF.

Unlike the draw solute loss (**Fig. 3**), DAP showed the highest maximum recovery followed by SOA, KNO_3 and CAN. This different trend between draw solute loss and maximum recovery rate was originated from their different dominant mechanisms. As we discussed above, draw solute loss was dominantly determined by both SRSF and recovery rate. However, maximum recovery rate was obtained from the extraction capacity of fertilizer DS which is affected by osmotic pressure of fertilizer DS. For example, as shown in **Eq. (4)**, if DS has high osmotic pressure at low concentration, its water extraction capacity will be high based on osmotic equillibrium and thus total recovery rate will be high. Similarly, since DAP has the highest osmotic pressure among fertilizers, DAP exhibitied the highest maximum recovery rate in spite of its high SRSF. Results from **Fig. 3** show that, to achieve low draw solute loss and high maximum recovery rate in FDFO, fertilizer DS should have low SRSF and high osmotic pressure.

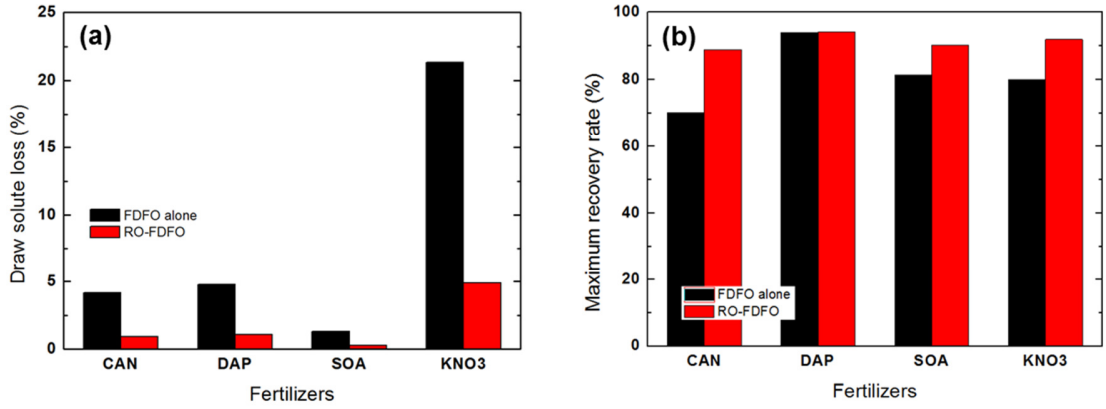

Figure 3. Comparative performances of FDFO and integrated RO-FDFO processes in terms of (a) draw solute loss and (b) maximum water recovery rate.

Compared to the FDFO process, the RO-FDFO hybrid process exhibited lower draw solute loss and higher maximum recovery rate with all fertilizers. In the RO-FDFO hybrid process, RO produced 75% of the feed as clean water while the FDFO process was used to further extract water only from the concentrate to increase the overall feed recovery rate to 95%. Therefore, the amount of the extracted water from the feed water by FDFO process in the hybrid system was lower than that in FDFO alone. As a result, the draw solute loss in the RO-FDFO hybrid process was much lower than that in FDFO. However, the RO-FDFO hybrid process exhibited higher maximum recovery rate than FDFO alone and this difference is likely induced by the difference of draw solute loss during the FDFO processes. In the FDFO process, the higher amount of draw solute was lost to the FS and thus the concentration of diluted DS could reached faster to its concentration that has equal osmotic pressure as the inital FS, resulting in a lower maximum recovery rate. It is very interesting to note that the trend of the maximum recovery rate between FDFO and the the RO-FDFO hybrid process was quite different. Although DAP showed the highest maximum recovery rates for both the processes however, other fertilizers showed a different trend. This is because, besides osmotic pressure, SRSF of the fertilizer DS is also an important factor for determining the maximum recovery rate. For example, as recovery rate increases, the loss of draw solute becomes more significant thereby accelerating the reduction of DS concentration resulting in a decrease in the maximum recovery rates. Therefore, by combining RO with FDFO, draw solute loss can be minimized and total recovery rate can be maximized.

424 The nutrient concentrations in the final FDFO product water were further simulated
425 in terms of major nutrients (N/P/K) using **Eq. (5)** to find out which process is more suitable
426 for producing favourable nutrient water for irrigation. Results shown in **Table 2** indicate
427 that KNO_3 in the FDFO process exhibited the lowest nitrogen concentration followed by
428 DAP, SOA and CAN since KNO_3 has the lowest nitrogen content (i.e., 13.85%) and the
429 highest draw solute loss (**Fig. 3a**). Although a loss in the draw solute could affect the
430 nutrient concentration however, the final DS concentration is mainly determined by
431 osmotic equilibrium with the initial FS concentration.

432

433 **Table 2**. Comparative performances of FDFO alone and the integrated RO-FDFO
434 processes in terms of N/P/K nutrient concentrations in the final FDFO product water.

Fertilizers	CAN	DAP		SOA	KNO_3	
Nutrients	N (mg/L)	N (ppm)	P (ppm)	N (ppm)	N (ppm)	K (ppm)
FDFO alone	268.40	201.19	222.45	230.63	114.76	320.33
RO-FDFO hybrid	199.25	186.55	206.26	194.31	93.98	262.34

435

436 When considering recommended concentrations (N/P/K) for beneficial plants (e.g.,
437 200/50/300 ppm for a tomato, 170/60/200 ppm for an eggplant and 200/50/200 ppm for a
438 cucumber) [16], **Table 2** indicates that the final product water from the FDFO process

439 could satisfy the recommended nitrogen concentration, however, still required substantial
440 dilution to reduce the phosphorous and potassium content.

441 Simulation results show that the RO-FDFO hybrid process has lower final nutrient
442 concentrations than the product water from the FDFO alone, making it more favourable for
443 direct fertigation. This was because, the FDFO process was used for treating only 25% of
444 the feed water in the form of RO brine and the further dilution was achieved by blending
445 the RO permeate and the diluted DS from the FDFO process. Although the RO-FDFO
446 hybrid process could reduce final nutrient concentration significantly and make more
447 favourable for fertigation compared to the FDFO process alone however, substantial
448 dilution is still required to meet the recommended concentration, especially in terms of
449 phosphorous nutrient concentraion. However, by controlling the composition of blended
450 fertilizers, the problem regarding exceeding the recommended concentrations can be solved
451 [16]. For example, if we consider a simple combination for only two different fertilizers
452 (i.e., DAP and KNO_3) with a molar ratio of 1:2.5, the final DS grade can achieve about
453 120/60/190 mg/L, which is quite suitable for growing an eggplant even though the
454 concentration of nutrients should be slightly adjusted. Based on the simulation results of
455 SEC and final nutrient concontrations, the RO-FDFO hybrid process can be considered as
456 the most suitable process for both CSG produced water treatment and favourable nutrient
457 water supply. Therefore, feasibility of the RO-FDFO hybrid process for treating CSG
458 produced water was further investigated in this study. Since CSG produced water treatment
459 by RO was already studied in the previous study [2], we focused on CSG RO brine

460 treatment by the 2nd stage FDFO process and assessed its performance in terms of water
461 flux, flux decline and the cleaning requirements.
462
463 ### 3.3 Flux decline in fertilizer-drawn forward osmosis during coal seam gas reverse
464 ### osmosis brine treatment
465 The FDFO experiments were carried out with CSG RO brine as FS and four
466 different fertilizers as DS under the AL-FS mode and their flux data is presented in the
467 form of normalized water flux in **Fig. 4**. KNO_3 exhibited the highest flux decline during 1
468 day operation followed by CAN, SOA and DAP. This is because FS conductivity with
469 KNO_3 was rapidly increased from 21.29 mS/cm to 40.9 mS/cm as presented in **Table S4**
470 due to its highest draw solute loss by RSF (**Table S3**) even though KNO_3 exhibited the
471 lowest accumulated permeate volume. The flux decline could also be caused by more
472 severer membrane fouling but based on the SEM images of the membrane surface with
473 KNO_3, it was observed that the membrane surface was only partially covered by foulant
474 deposits as shown in **Fig. 5d**. Thus, it can be concluded that the severest flux decline with
475 KNO_3 is due to significant decrease in the osmotic driving force caused by the loss of draw
476 solutes towards the FS.
477

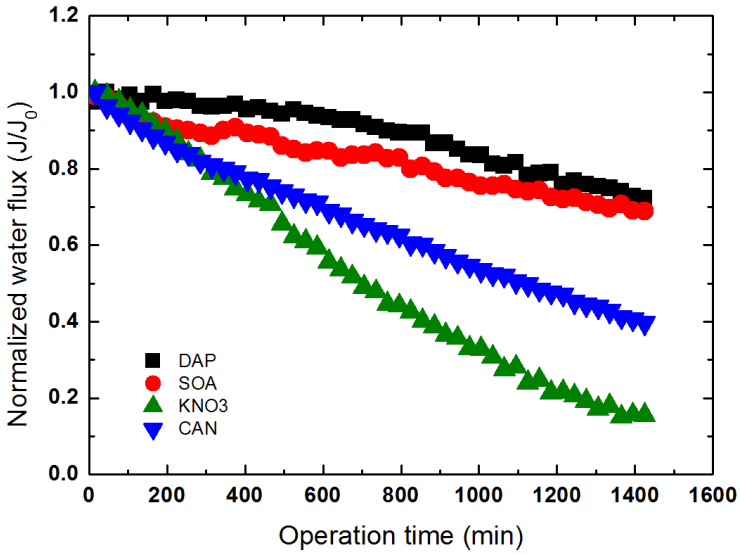

478

479 **Figure 4**. Flux-decline curves obtained during FO experiments with four different fertilizer
480 DS. Experimental conditions of all FO experiments: CSG RO brine as FS; four different
481 fertilizers as DS; crossflow velocity of 8.5 cm/s; and temperature of 25 ± 1 °C. All FDFO
482 experiments were conducted repeatedly.

483

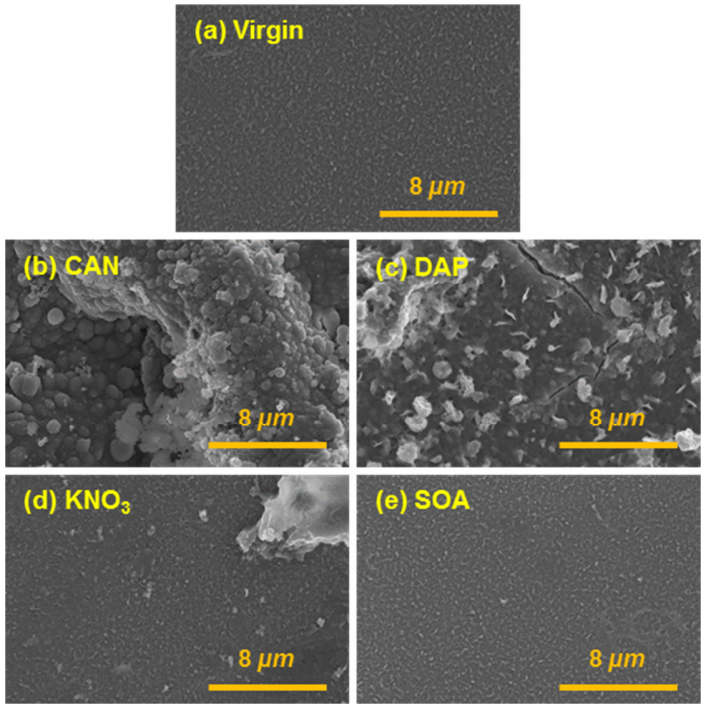

Figure 5. SEM images of (a) virgin membrane and fouled membrane with of (b) CAN DS, (c) DAP DS, (d) KNO_3 DS and (e) SOA DS.

CAN exhibited the second highest flux decline which is likey due to both an increase in salinity in the FS and membrane fouling. **Table S4** showed that FS conductivity with CAN significantly increased from 20.63 mS/cm to 31.6 mS/cm, resulting in a reduction in the concentration gradient between FS and DS. In addition, **Fig. 5b** revealed that the surface of FO membrane with CAN was covered by thick scaling layer, the likely main cause of the severe flux decline. When comparing SOA with DAP, it is interesting to note that DAP exhibited lower flux decline even though severer membrane fouling seems to have occurred on the membrane surface with DAP as shown in **Fig. 5c**. As shown in **Fig. 5e,** no apparent fouling layer was however observed on the membrane surface with SOA as

497 DS. A lower flux decline with DAP as DS may be due to lower feed recovery rate with
498 DAP as its FS conductivity increased only slightly from 20.84 mS/cm to 26.3 mS/cm while
499 that with SOA increased from 20.58 mS/cm to 28.5 mS/cm.

500 From these results, it can be concluded that an increase in FS concentration (batch
501 process) and a decrease in DS concentration due to the loss by RSF were the dominant
502 factor affecting the flux decline in the FDFO process even though membrane fouling layer
503 was formed on the membrane surface with some fertilizers. It is interesting to compare
504 experimental SRSF without a fouling layer with the change in the FS conductivity in terms
505 of specific conductivity increment which is defined as a ratio of the difference between
506 initial and final conductivities to accumulated permeate volume. KNO_3 showed the highest
507 specific FS conductivity increment followed by CAN, SOA and DAP, while KNO_3
508 exhibited the highest SRSF followed by CAN, DAP, SOA. KNO_3 and CAN showed the
509 similar trend since they had very high SRSF while on the other hand, DAP and SOA with
510 quite low SRSF had the different trend, implying that the fouling layer can have an impact
511 on reducing SRSF in FDFO.

512 To identify the scaling layer formed on the membrane surface with a variety of
513 fertilizer DS, XRD analysis was carried out on the fouled/scaled membrane surface and
514 presented in **Fig. 6a**. Results show that the membrane with KNO_3 and SOA has similar
515 XRD peaks to the virgin membrane, indicating that no scaling layer was formed on the
516 membrane surface, consistent with SEM analysis results (**Fig. 5d and 5e**). As shown in
517 **Table 1**, CSG RO brine is composed of various scaling precursors including calcium,
518 magnesium, phosphate and carbonate ions, indicating that CSG RO brine has high scaling

519 potential. Thus, membrane scaling can be formed on the membrane surface when CSG RO
520 brine is highly concentrated [35]. Furthermore, since KNO_3 and SOA did not contain any
521 scaling precursor, RSF could not affect membrane scaling formation as depicted in **Fig. 7a**.
522

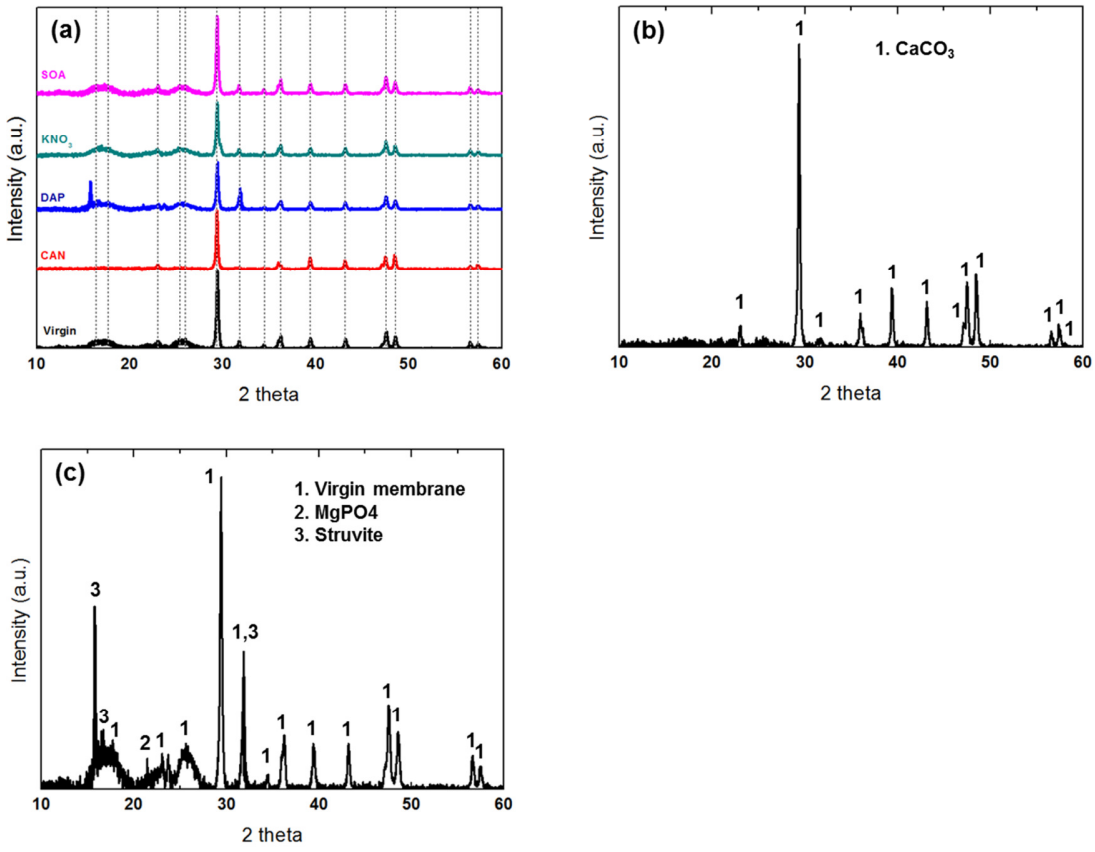

523
524

525 **Figure 6**. XRD patterns of virgin and fouled membranes: (a) comparison of XRD peaks
526 between virgin membrane and fouled membranes with four different fertilizer DS, (b)
527 comparison of XRD peaks between fouled membranes with CAN and $CaCO_3$ crystal, and
528 (c) comparison of XRD peaks between fouled membranes with DAP, magnesium
529 phosphate, and magnesium ammonium phosphate (struvite).
530

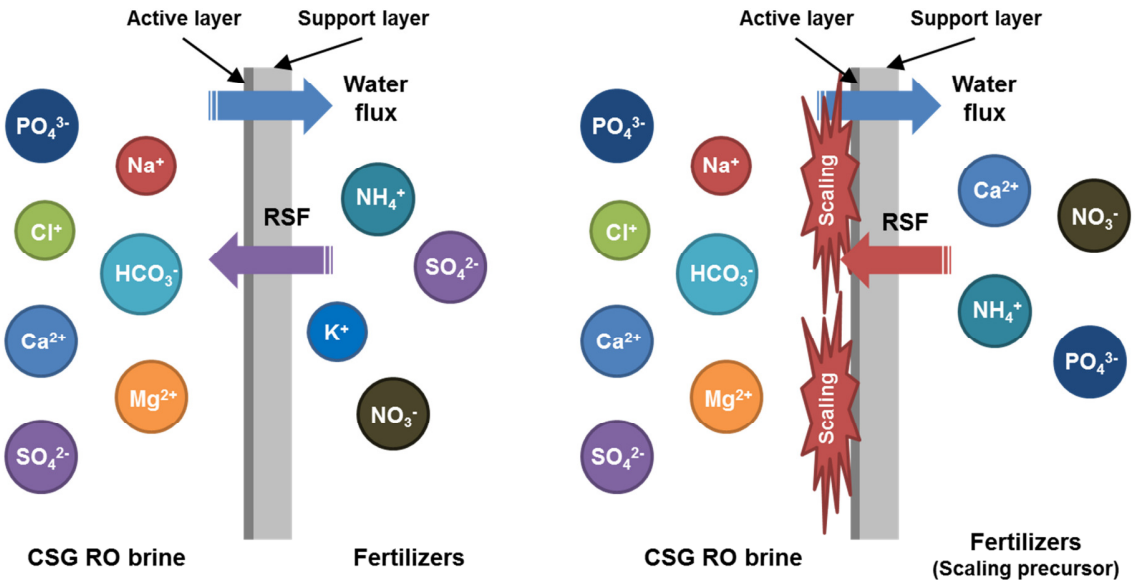

Figure 7. Schematic description of FO membrane fouling/scaling during CSG RO brine treatment by FDFO: (a) fertilizers (i.e., SOA and KNO_3) without scaling precursors, and (b) fertilizers (i.e., CAN and DAP) with scaling precursors.

On the other hand, the XRD pattern for the membrane surface with DAP and CAN exhibited slightly different peaks compared to the virgin FO membrane. For FO membrane used with CAN, most XRD peaks were identical to virgin membrane but some peaks were not visible and some new peaks appeared suggesting that these XRD peaks likely originated from the membrane scaling layer, not the membrane surface. Since calcium was found from EDX analysis (data not shown), XRD peaks with CAN were compared with reference peaks of calcium carbonate (**Fig. 6b**) which agreed very well indicating the presence of $CaCO_3$ scaling on the membrane surface. Since magnesium and phosphorous were also found from EDX analysis (data not shown), XRD peaks with DAP were also compared with reference peaks of magnesium phosphate and struvite (**Fig. 6c**). Results

546 agreed with struvite, indicating that the scaling layer was primarily composed of struvite.
547 These results suggested that the membrane scaling is significantly affected by draw solute
548 containing scaling precursors such as calcium and phosphate as shown in **Fig. 7b**. Due to
549 the high concentration gradient, draw solute with a scaling precursor can pass through FO
550 membrane and accelerate ions concentration on the membrane surface [36]. If this exceeds
551 its solubility limits such as of calcium carbonate, magnesium phosphate and struvite, it
552 results in the formation of scales on the membrane surface contributing to flux decline.
553 Besides, the reversely diffused draw solutes can interact with certain ions in FS and induce
554 the formation of a scaling layer [37]. As a result, calcium carbonate and struvite were
555 dominantly formed on the membrane surface with CAN and DAP, respectively.

556 It is very interesting to note that struvite was formed on the FO membrane with
557 DAP DS rather than $Ca_3(PO_4)_2$ and $Mg_3(PO_4)_2$ even though their solubility product
558 constants are much lower than struvite. Ca^{2+}, Mg^{2+} and PO_4^{3-} ions are required for the
559 formation of $Ca_3(PO_4)_2$ and $Mg_3(PO_4)_2$, while HPO_4^{2-}, Mg^{2+} and NH_4^+ ions are required for
560 the struvite formation ($MgNH_4PO_4$) [20]. However, NH_4^+ and HPO_4^{2-} ions are the dominant
561 species of DAP DS, resulting in their high reverse diffusion to FS. Consequently, struvite is
562 likely formed on the FO membrane with DAP as DS. As well as the effect of RSF on the
563 scaling formation in FS, FSF also can influence the complexation with DS. However, FSF
564 in FDFO is very low compared to other desalting membrane processes (e.g., NF or RO) due
565 to the hindrance effect of RSF on FSF [38]. Thus, the effect of FSF will be very limited.
566 Besides, although the complexation of FS with DS occurs, it can hardly affect the FO
567 performance due to the permeate flow direction from FS to DS.

568

569 **3.4 Strategy for controlling membrane fouling**

570 The results of membrane physical cleaning show that the water fluxes were fully
571 recovered for FO membrane used with KNO_3 and SOA, which are consistent with SEM
572 results (Fig. 8a). **Fig S2c and S2d** indicated that the membrane fouling layer formed on the
573 active layer could be readily removed by physical or hydraulic washing. This is because, as
574 previously discussed, KNO_3 and SOA have low scaling potential while CAN and DAP
575 exhibited less than 90% water flux recovery. These poor flux recovery rates (i.e., 82.3%
576 and 86.6%, respectively) of FO membrane operated with CAN and DAP show that physical
577 or hydraulic washing was not effective in removing the membrane foulants formed on the
578 active layer. **Fig. S2a and S2b** confirmed that the membrane fouling layer still remained on
579 the active layer with CAN and DAP.

580

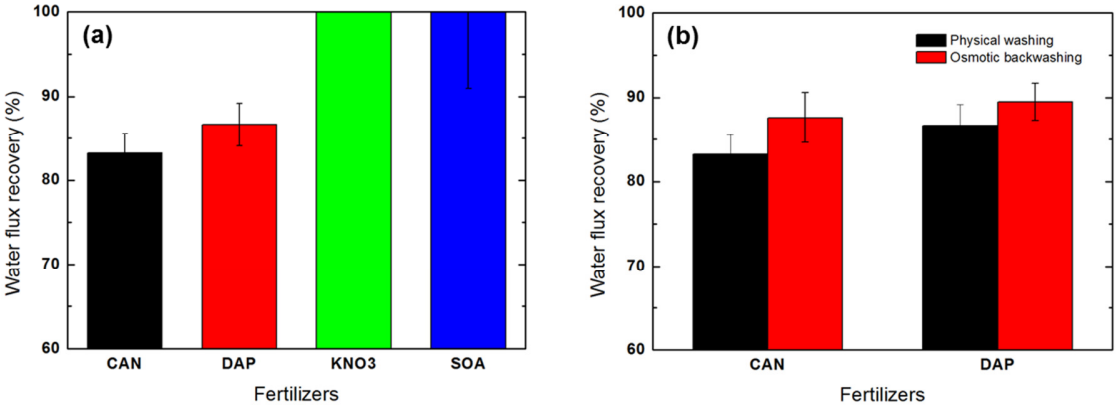

581

582 **Figure 8**. Water flux recovery after (a) hydraulic washing and (b) osmotic backwashing.
583 Experimental conditions for hydraulic washing: DI water as FS and DS; crossflow velocity
584 of 25.5 cm/s; cleaning duration of 30 min; and temperature of 25 ± 1 °C. Experimental

585 conditions for osmotic backwashing: 1M NaCl as FS; DI water as DS; crossflow velocity
586 of 8.5 cm/s; cleaning duration of 30 min; and temperature of 25 ± 1 °C.
587
588 In order to further enhance water flux recovery, osmotic backwashing was applied
589 for the fouled FO membrane with CAN and DAP using DI water on the active layer and 1
590 M NaCl on the support layer side at the same crossflow velocity (i.e., 8.5 cm/s for 30
591 minutes). **Fig. 8b** shows that water flux recovery was slightly enhanced compared to the
592 hydraulic washing. However, **Fig S2e and S2f** indicate that the fouling layer on the
593 membrane surface could not be completely removed, which is consistent with the water
594 flux recovery results. The results of the osmotic backwashing agreed well with other studies
595 [19]. However, the results of physical cleaning experiments and SEM images showed that
596 FO membranes with CAN and DAP still require further cleaning.
597 Chemical cleaning was further investigated for the complete removal of the
598 fouling/scaling layer using three different chemicals (EDTA 1mM, NaOH 1mM and citric
599 acid 1%), and the results are presented in **Fig. 9a**. The fouled FO membrane with CAN was
600 utilized for this study since CAN showed the most severe membrane fouling as well as high
601 flux decline. **Fig. 9a** demonstrated that 1% citric acid was more efficienct for recovering
602 water flux compared to the other chemicals (i.e., EDTA 1mM and NaOH 1mM). Moreover,
603 SEM images (**Fig. S3d**) showed that the fouling layer structure was slightly changed by
604 exposure to citric acid 1%. Citric acid is a weak acid which can dissolve inorganic minerals
605 and be utilized for removing the scaling layer [39]. In addition, citric acid is widely utilized

as a chelating agent [40]. Therefore, this can lead to complex with Ca^{2+} ions, resulting in a reduction of scaling on the membrane surface.

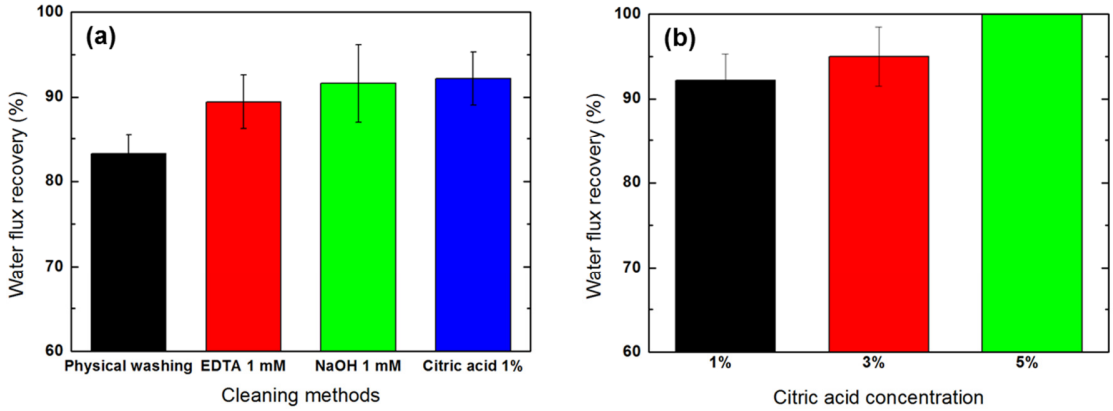

Figure 9. Water flux recovery of fouled membrane with CAN after chemical cleaning with (a) varying chemical agents (i.e., EDTA 1 mM, NaOH 1 mM and citric acid 3%) and (b) increasing citric acid concentration. Experimental conditions for chemical cleaning: testing chemical agents as FS; DI water as DS; crossflow velocity of 8.5 cm/s; cleaning duration of 30 min; and temperature of 25 ± 1 °C.

Interestingly, 1 mM EDTA and 1 mM NaOH showed better cleaning efficiency than hydraulic washing. EDTA is generally utilized for distrupting the fouling layer structure through a ligand exchange between EDTA and organic-divalent complexes [26]. Therefore, 1 mM EDTA was effective for removing calcium carbonate scaling, resulting in an increase in water flux recovery [19]. However, **Fig. S3b** shows that 1 mM EDTA could not remove the scaling layer. NaOH has been used for dissolving organic foulants in basic solution [27], but it was efficient for recoverying water flux even though the major fouling mechanism

623 was membrane scaling enhanced by RSF. This is because CSG RO brine was a mixture of
624 organics and inorganics as shown in **Table 1**, which can accelerate membrane fouling due
625 to synergistic effects by combined organic–inorganic fouling [41]. Thus, NaOH could
626 enhance water flux recovery by disolving organics from the combined fouling layer.
627 However, **Fig. S3c** indicates that the effect of NaOH on membrane cleaning efficiency is
628 limited.

629 To further enhance the cleaning efficiency, chemical cleanings were carried out by
630 increasing the citric acid concentration. By increasing the citric acid concentration from 1 %
631 to 3 %, the water flux recovery was slightly enhanced (**Fig. 9b**) and **Fig. S3e** indicates that
632 there was still some scaling layers on the membrane surface. When the citric acid
633 concentration was further increased to 5%, water flux was perfectly recovered as shown in
634 **Fig. 9b** and this was confirmed in **Fig. S3f** which demonstrates that the fouling layer was
635 completely removed. Since citric acid 5% exhibited the most efficient cleaning efficiency,
636 fouled FO membrane with DAP was also assessed for its cleaning efficiency using 5%
637 citric acid as chemical cleaning agent As shown in **Fig S3h**, it was observed that the
638 membrane surface was completely cleaned as well as water flux was fully recovered (data
639 not shown) with 5% citric acid chemical cleaning.

640

641**4. Conclusions**

642 In this study, three processes (i.e., RO alone, FDFO alone and the RO-FDFO hybrid
643 process) in terms of SEC and nutrient concentrations in the final FDFO product water were
644 evaluated and compared. Membrane fouling in FDFO during CSG RO brine treatment was

645 then investigated and the strategies of controlling membrane fouling were also assessed.
646 The primary findings drawn from this study are summarized as follows:

647 • SEC analysis showed that FDFO alone has the lowest SEC followed by the RO-
648 FDFO hybrid process and RO alone.
649 • Simulation of the final nutrient concentration suggested that the RO-FDFO hybrid
650 system can achieve lower final concentration, higher maximum recovery and lower
651 nutrient loss compared to FDFO process alone.
652 • From both SEC analysis and final nutrient simulation, it can be drawn that the RO-
653 FDFO hybrid process is the most promising process for both CSG RO brine
654 treatment and favorable nutrient supply.
655 • During CSG RO brine treatment, KNO_3 exhibited the highest flux decline than
656 other fertilizers since FS concentration was highly increased due to high RSF.
657 • CAN showed the most severe membrane scaling caused by reversely transported
658 calcium ions to FS.
659 • To control membrane fouling in the FDFO process, citric acid cleaning was the
660 most effective chemical agent for chemical cleaning.

661

662 **Acknowledgements**

663 This research was supported by a grant (code 16IFIP-B088091-03) from Industrial
664 Facilities & Infrastructure Research Program funded by Ministry of Land, Infrastructure
665 and Transport of Korean government.

666

667 **References**

668 [1] T.A. Moore, Coalbed methane: A review, International Journal of Coal
669 Geology, 101 (2012) 36-81.

670 [2] L.D. Nghiem, C. Elters, A. Simon, T. Tatsuya, W. Price, Coal seam gas
671 produced water treatment by ultrafiltration, reverse osmosis and multi-
672 effect distillation: A pilot study, Separation and Purification Technology,
673 146 (2015) 94-100.

674 [3] L.D. Nghiem, T. Ren, N. Aziz, I. Porter, G. Regmi, Treatment of coal
675 seam gas produced water for beneficial use in Australia: A review of best
676 practices, Desalination and Water Treatment, 32 (2011) 316-323.

677 [4] G.J. Millar, S.J. Couperthwaite, K. Alyuz, Behaviour of natural zeolites
678 used for the treatment of simulated and actual coal seam gas water,
679 Journal of Environmental Chemical Engineering, 4 (2016) 1918-1928.

680 [5] H. Zhao, G.F. Vance, M.A. Urynowicz, R.W. Gregory, Integrated
681 treatment process using a natural Wyoming clinoptilolite for remediating
682 produced waters from coalbed natural gas operations, Applied Clay
683 Science, 42 (2009) 379-385.

684 [6] H. Lee, Y. Jin, S. Hong, Recent transitions in ultrapure water (UPW)
685 technology: Rising role of reverse osmosis (RO), Desalination, 399 (2016)
686 185-197.

687 [7] T.H. Chong, S.-L. Loo, W.B. Krantz, Energy-efficient reverse osmosis
688 desalination process, Journal of Membrane Science, 473 (2015) 177-188.

689 [8] S. Liang, C. Liu, L. Song, Two-Step Optimization of Pressure and
690 Recovery of Reverse Osmosis Desalination Process, Environmental
691 Science & Technology, 43 (2009) 3272-3277.

692 [9] Y. Kim, S. Lee, J. Kuk, S. Hong, Surface chemical heterogeneity of
693 polyamide RO membranes: Measurements and implications, Desalination,
694 367 (2015) 154-160.

[10] T.Y. Cath, A.E. Childress, M. Elimelech, Forward osmosis: Principles, applications, and recent developments, Journal of Membrane Science, 281 (2006) 70-87.

[11] L. Chekli, S. Phuntsho, J.E. Kim, J. Kim, J.Y. Choi, J.-S. Choi, S. Kim, J.H. Kim, S. Hong, J. Sohn, H.K. Shon, A comprehensive review of hybrid forward osmosis systems: Performance, applications and future prospects, Journal of Membrane Science, 497 (2016) 430-449.

[12] M. Xie, L.D. Nghiem, W.E. Price, M. Elimelech, A Forward Osmosis–Membrane Distillation Hybrid Process for Direct Sewer Mining: System Performance and Limitations, Environmental Science & Technology, 47 (2013) 13486-13493.

[13] T.N. Bitaw, K. Park, D.R. Yang, Optimization on a new hybrid Forward osmosis-Electrodialysis-Reverse osmosis seawater desalination process, Desalination, 398 (2016) 265-281.

[14] S. Phuntsho, S. Hong, M. Elimelech, H.K. Shon, Forward osmosis desalination of brackish groundwater: Meeting water quality requirements for fertigation by integrating nanofiltration, Journal of Membrane Science, 436 (2013) 1-15.

[15] S. Phuntsho, H.K. Shon, S. Hong, S. Lee, S. Vigneswaran, A novel low energy fertilizer driven forward osmosis desalination for direct fertigation: Evaluating the performance of fertilizer draw solutions, Journal of Membrane Science, 375 (2011) 172-181.

[16] S. Phuntsho, H.K. Shon, T. Majeed, I. El Saliby, S. Vigneswaran, J. Kandasamy, S. Hong, S. Lee, Blended Fertilizers as Draw Solutions for Fertilizer-Drawn Forward Osmosis Desalination, Environmental Science & Technology, 46 (2012) 4567-4575.

[17] Y. Kim, L. Chekli, W.-G. Shim, S. Phuntsho, S. Li, N. Ghaffour, T. Leiknes, H.K. Shon, Selection of suitable fertilizer draw solute for a novel fertilizer-drawn forward osmosis–anaerobic membrane bioreactor hybrid system, Bioresource Technology, 210 (2016) 26-34.

[18] C. Boo, S. Lee, M. Elimelech, Z. Meng, S. Hong, Colloidal fouling in forward osmosis: Role of reverse salt diffusion, Journal of Membrane Science, 390–391 (2012) 277-284.

[19] S. Lee, Y.C. Kim, Calcium carbonate scaling by reverse draw solute diffusion in a forward osmosis membrane for shale gas wastewater treatment, Journal of Membrane Science, 522 (2017) 257-266.

[20] Y. Kim, S. Li, L. Chekli, Y.C. Woo, C.-H. Wei, S. Phuntsho, N. Ghaffour, T. Leiknes, H.K. Shon, Assessing the removal of organic micro-pollutants from anaerobic membrane bioreactor effluent by fertilizer-drawn forward osmosis, Journal of Membrane Science, 533 (2017) 84-95.

[21] Y. Kim, S. Li, L. Chekli, S. Phuntsho, N. Ghaffour, T. Leiknes, H.K. Shon, Influence of fertilizer draw solution properties on the process performance and microbial community structure in a side-stream anaerobic fertilizer-drawn forward osmosis – ultrafiltration bioreactor, Bioresource Technology.

[22] R. Taddeo, K. Kolppo, R. Lepistö, Sustainable nutrients recovery and recycling by optimizing the chemical addition sequence for struvite precipitation from raw swine slurries, Journal of Environmental Management, 180 (2016) 52-58.

[23] A. Tiraferri, N.Y. Yip, A.P. Straub, S. Romero-Vargas Castrillon, M. Elimelech, A method for the simultaneous determination of transport and structural parameters of forward osmosis membranes, Journal of Membrane Science, 444 (2013) 523-538.

[24] Y.C. Woo, Y. Chen, L.D. Tijing, S. Phuntsho, T. He, J.-S. Choi, S.-H. Kim, H.K. Shon, CF4 plasma-modified omniphobic electrospun nanofiber membrane for produced water brine treatment by membrane distillation, Journal of Membrane Science, 529 (2017) 234-242.

[25] Y. Kim, S. Lee, H.K. Shon, S. Hong, Organic fouling mechanisms in forward osmosis membrane process under elevated feed and draw solution temperatures, Desalination, 355 (2015) 169-177.

[26] S. Hong, M. Elimelech, Chemical and physical aspects of natural organic matter (NOM) fouling of nanofiltration membranes, Journal of Membrane Science, 132 (1997) 159-181.

[27] W.S. Ang, S. Lee, M. Elimelech, Chemical and physical aspects of cleaning of organic-fouled reverse osmosis membranes, Journal of Membrane Science, 272 (2006) 198-210.

[28] Y.C. Woo, J.J. Lee, L.D. Tijing, H.K. Shon, M. Yao, H.-S. Kim, Characteristics of membrane fouling by consecutive chemical cleaning in pressurized ultrafiltration as pre-treatment of seawater desalination, Desalination, 369 (2015) 51-61.

[29] Y.C. Woo, Y. Kim, W.-G. Shim, L.D. Tijing, M. Yao, L.D. Nghiem, J.-S. Choi, S.-H. Kim, H.K. Shon, Graphene/PVDF flat-sheet membrane for the treatment of RO brine from coal seam gas produced water by air gap membrane distillation, Journal of Membrane Science, 513 (2016) 74-84.

[30] A. Altaee, G. Zaragoza, H.R. van Tonningen, Comparison between Forward Osmosis-Reverse Osmosis and Reverse Osmosis processes for seawater desalination, Desalination, 336 (2014) 50-57.

[31] S. Phuntsho, S. Hong, M. Elimelech, H.K. Shon, Osmotic equilibrium in the forward osmosis process: Modelling, experiments and implications for process performance, Journal of Membrane Science, 453 (2014) 240-252.

[32] J.R. McCutcheon, M. Elimelech, Influence of concentrative and dilutive internal concentration polarization on flux behavior in forward osmosis, Journal of Membrane Science, 284 (2006) 237-247.

[33] N.M. Mazlan, D. Peshev, A.G. Livingston, Energy consumption for desalination — A comparison of forward osmosis with reverse osmosis, and the potential for perfect membranes, Desalination, 377 (2016) 138-151.

[34] J.R. McCutcheon, M. Elimelech, Influence of membrane support layer hydrophobicity on water flux in osmotically driven membrane processes, Journal of Membrane Science, 318 (2008) 458-466.

786 [35] H.C. Duong, S. Gray, M. Duke, T.Y. Cath, L.D. Nghiem, Scaling control
787 during membrane distillation of coal seam gas reverse osmosis brine,
788 Journal of Membrane Science, 493 (2015) 673-682.

789 [36] S. Lee, C. Boo, M. Elimelech, S. Hong, Comparison of fouling behavior
790 in forward osmosis (FO) and reverse osmosis (RO), Journal of Membrane
791 Science, 365 (2010) 34-39.

792 [37] Z. Li, R. Valladares Linares, S. Bucs, C. Aubry, N. Ghaffour, J.S.
793 Vrouwenvelder, G. Amy, Calcium carbonate scaling in seawater
794 desalination by ammonia–carbon dioxide forward osmosis: Mechanism
795 and implications, Journal of Membrane Science, 481 (2015) 36-43.

796 [38] C. Kim, S. Lee, H.K. Shon, M. Elimelech, S. Hong, Boron transport in
797 forward osmosis: Measurements, mechanisms, and comparison with
798 reverse osmosis, Journal of Membrane Science, 419–420 (2012) 42-48.

799 [39] E. Filloux, J. Wang, M. Pidou, W. Gernjak, Z. Yuan, Biofouling and
800 scaling control of reverse osmosis membrane using one-step cleaning-
801 potential of acidified nitrite solution as an agent, Journal of Membrane
802 Science, 495 (2015) 276-283.

803 [40] Y. Zhao, L. Jia, K. Liu, P. Gao, H. Ge, L. Fu, Inhibition of calcium sulfate
804 scale by poly (citric acid), Desalination, 392 (2016) 1-7.

805 [41] Y. Kim, M. Elimelech, H.K. Shon, S. Hong, Combined organic and
806 colloidal fouling in forward osmosis: Fouling reversibility and the role of
807 applied pressure, Journal of Membrane Science, 460 (2014) 206-212.

808